SEMARAK ILMU PUBLISHING

Journal of Advanced Research in Numerical Heat Transfer

Journal homepage:
https://semarakilmu.com.my/journals/index.php/arnht/index
ISSN: 2735-0142

Aligned Magnetohydrodynamics and Thermal Radiation Effects on Ternary Hybrid Nanofluids Over Vertical Plate with Nanoparticles Shape Containing Gyrotactic Microorganisms

Siti Shuhada Ishak[1], Fazillah Bosli[2], Seripah Awang Kechil[1], Mohd Rijal Ilias[1,*]

[1] School of Computing, Informatics and Mathematics, Universiti Teknologi MARA, 40450 Shah Alam, Selangor, Malaysia
[2] College of Computing, Informatics and Mathematics, Universiti Teknologi MARA (UiTM) Kedah Branch, Sungai Petani Campus, Merbok, Kedah, Malaysia

ARTICLE INFO

Article history:
Received 8 December2023
Received in revised form 10 January 2024
Accepted 9 Februrary 2024
Available online 30 March 2024

Keywords:
Gyrotactic microorganisms; Ternary Hybrid Nanofluids; Nanoparticles shape; Magnetohydrodynamics; Radiation; Vertical plate

ABSTRACT

Nowadays, challenges in development of heat transfer for various engineering fields including heat exchangers, electronics, chemical and bio-industry and others are crucial. Ternary hybrid nanofluids (THNF) as a new heat transfer liquids can be considered as effective medium for increment of heat and energy transport. In the case of THNF when three nanoparticles are added in the based fluid to enhance the transport processes. Dissimilar to the nanofluids (NF) and hybrid nanofluids (HNF) model that considers two types of nanoparticles, this studied consider the three types of nanoparticles in this work which are Aluminium Oxide (Al_2O_3), Copper (Cu), and Carbon Nanotube (CNT) with different shapes containing gyrotactic microorganisms. The objective is to find the effect of magnetohydrodynamics (MHD) and radiation to the steady of THNF flow past the vertical plate. The mathematical model has been formulated based on a combination Tiwari-Das and Buongiorno nanofluids model. The governing flow and heat transfer equations are simplified to the ordinary differential equations (ODEs) with the adaptation of conventional similarity transformations which are then evaluated by the bvp4c solver (MATLAB) to generate the numerical solutions. The solutions are visually represented through graphs and table to be easily observed. The results indicated that the effect of magnetic field parameter (M) decrease the velocity and contrary in concentration, and microorganism profile while the temperature is increased in magnetic but contrary in radiation parameter (Rd). The concentration and density microorganism of THNF is increase with higher value in Rd and M but decrease in velocity and temperature. The spherical nanoparticle shape has a higher density, causing the skin friction of THNF to be lower compared to NF and HNF.

1. Introduction

In recent times, further extension of hybrid nanofluid has led to the disseminating of three types of nanoparticles in a base fluid to synthesize a colloidal suspension termed a THNF which holds

* *Corresponding author.*
E-mail address: mrijal@uitm.edu.my (Mohd Rijal Ilias)

https://doi.org/10.37934/arnht.18.1.6891

exceptional thermal abilities as compared to HNF or usual NF. The potency of THNF is predicted by the type and size of nanoparticles, and their mixing ratio. This new sort of nanofluids has a variety of fabulous utilities in engineering and industrial sectors, e.g., petroleum reservoirs, nuclear cooling systems, modern electronics cooling, aerospace technology, laser technology, medical instruments, pharmaceutical manufacturing, etc. [1]. The enhanced thermal conductivity of nanofluids can be associated with various factors, including particle shape and size, material composition, and volume fraction [2-3]. The different shapes of tiny particles have differences in the interactions and agglomeration, and host fluids are associated with surface charges. The colloidal combination of three different types of tiny particles of nanoparticles subject to one base fluid and the trihybrid nanofluid has started with the results of a couple of investigations appear to be insightful and encouraging [4]. The heat transfer in the base fluid was enhanced due to various shapes of nano-sized particles [5] and trihybrid fluid temperatures were higher compared to the single and two-type nanoparticle suspensions with base fluids [6]. In a study carried out by Manjunatha *et al.,* [7], they introduced a novel theoretical model for THNFs, mathematically defining properties such as specific heat capacity, electrical conductivity, thermal conductivity, viscosity, and density. Their research revealed that THNFs exhibit superior thermal conductivity compared to HNFs. In a different study, Ramzan *et al.,* [8] deduced that the heat transfer rate of THNFs outperformed silver nanofluids by 46%. This observation was based on their investigation of kerosene-based THNF flow, incorporating silver, copper, and graphene oxide nanoparticles.

The shape of nanoparticles in THNFs can have a significant impact on their dispersion, stability, and how they interact with both the base fluid and additives. Various shapes, including spheres, rods, plates, and other geometries, possess distinct surface area-to-volume ratios. These differences can influence properties such as thermal conductivity, optical characteristics, and responsiveness to radiation. Additionally, nanoparticle shape can affect their behavior in the presence of external fields, such as magnetic forces. While spherical nanoparticles are commonly used by most researchers, they have limitations in terms of their applications and significance. Adun *et al.,* [9] and Sahoo [10] delved into the influence of nanoparticle shapes, material, size, and nanofluid proportions on optimizing the properties of THNFs. Sahoo [11] further validated the concept of THNF through numerical flow analysis experiments, investigating its potential as an effective coolant in industrial heat transfer applications. Animasaun *et al.,* [12] explored convective heating in the transportation of THNFs of various shapes. They found that harnessing convective heating could result in a significantly elevated heat transfer rate. Similarly, Raju *et al.,* [13] employed simple linear regression to clarify the nonlinear movements of axisymmetric THNFs with varying shapes and densities. Their findings indicated higher temperature distribution while contrasting results were observed in the momentum boundary layer. Shanmugapriya *et al.,* [14] discussed THNFs with various nanoparticle shapes and found that blade-shaped ternary hybrid nanoparticles exhibited a greater tendency to enhance heat transfer rates compared to those with platelets, cylinders, bricks, and spherical shapes. Elnaqeeb *et al.,* [15] investigated the large nanoparticle density (i.e., copper oxide, copper, and silver) with different shapes to the effect of the local skin friction, heat transfer, and the dynamics of water based ternary hybrid nanofluids. They found that the temperature distribution is maxima while heat transfer is minima in the case of ternary-hybrid nanofluids. The previous studies on the shape of nanoparticle in different situation such as [16-17].

The flow of gyrotactic microbes in nanofluids has acquired much attention among scientists and research community due to its employments in several areas of bio-technology and science. The benefits of including nanoparticles in mobile microbes' suspension can be found in microvolumes, microscale mixing and nanofluid stability [18]. Microorganisms are used to prepare the industrial and commercial items like biofuel, biofertilizers and bioactive secondary metabolite (alcohol) etc. Algae

(one of the microorganisms) are fast growing biomass and can be converted to biodiesel fuel or biofuel [19]. The interplay between motile microorganisms and nanoparticles, coupled with buoyancy forces, leads to the generation of bioconvection in nanofluids. Typically, bioconvection flow involves single-cell microorganisms like algae and bacteria. The orientation of motile microorganisms as they swim is governed by the equilibrium between two torques: one arising from the viscous drag force induced by shear flow and the other from the influence of gravity when these microorganisms are within a flow field [20]. Khan *et al.,* [21] investigated the natural convection boundary-layer flow of a water-based nanofluids containing gyrotactic microorganisms and found that density number of motile microorganisms, Sherwood number, Nusselt number and skin friction increase along the surface. The impact of gyrotactic microorganisms of Cu-Al_2O_3/water hybrid nanofluid towards an immovable plate is numerically examined by Khashi'ie *et al.,* [22] and concluded that the hybrid nanofluids of heat and mass transfer rates including the density of microorganisms is higher than the nanofluids. Yaseen *et al.,* [23] examined the bioconvection phenomenon in a THNF flow that included motile gyrotactic microorganisms. Their research revealed that as the bioconvection Lewis number increased, there was a corresponding decrease in the microorganism concentration profile. Algehyne *et al.,* [24] conducted an analysis using the Buongiorno model to study mass and energy transmission in trihybrid nanofluids flow, without the inclusion of microorganisms. They concluded that trihybrid nanofluids demonstrated a remarkable enhancement in the rate of energy propagation when compared to simple and hybrid nanofluids.

The study of MHD of boundary layer flow with heat and mass transfer of boundary layer flow can be of great benefit to the industrial of the engineering processes occur at a high temperature such as in nuclear power plants, gas turbines and various propulsion devices for aircraft, missiles, satellites, and space vehicles. The effect of magnetic field on various scenarios and consistently observed that the magnetic field's influence enhances heat transfer and fluid velocity was studied by many researchers referenced in [25–27]. The interaction between a magnetic field and electrically conducting liquids significantly impacts boundary layer control. In studied by Vajravelu and Nayfeh [28] elucidated that the boost of magnetic field strength causes a reduction in velocity due to the intensified Lorentz force, which opposes the flow and results in deceleration. Their result is aligned with the predictions since the magnetic field imposes a decelerating effect on the convective flow. Batool and Ashraf [29] investigated the impact of a magnetic field on bioconvection flow, noting that the applied magnetic field tends to increase shear stress while decreasing rates of heat transfer, nanoparticle volume fraction, and microorganism density. Alharbi *et al.,* [30] delved into hybrid nanofluid flow involving gyrotactic microorganisms under the influence of an induced magnetic field. Their findings indicated that an increase in the magnetic field parameter led to decreased velocity profiles. Asjad *et al.,* [31] explored bioconvection in the presence of a magnetic field and discovered that the velocity profile increased, along with temperature, as a function of the magnetic parameter. Soid *et al.,* [22] studied gyrotactic microorganisms in the presence of a magnetic field, incorporating Copper (Cu) and Aluminium Oxide (Al_2O_3) nanoparticles in water. Mahmood *et al.,* [33] studied the MHD effect on THNFs with cylindrical-shaped nanoparticles. They found that the magnetic field increased velocity but had the opposite effect on the nanoparticle volume fraction parameter. THNFs exhibited enhanced heat transfer rates and exerted a greater influence on surfaces compared to hybrid and regular nanofluids. Others researcher study on magnetic impact in the various problem such as [34-37].

Several researchers, as referenced in [38-40], have investigated the effect of radiation on MHD under different conditions. They found that radiation tends reduce the velocity while increase the temperature. Dolui *et al.,* [41] examined THNFs with radiation effects in the presence of MHD and noted that magnetic forces significantly influence flow velocity while the increment of radiation

parameter produces the opposite effect. Jakeer *et al.,* [42] studied the impact of MHD flow with thermal radiation on a couple stress water-based NFs, HNFs, and THNFs. They discovered that increasing the inertia coefficient leads to reduced velocity, but oppositely for the temperature in THNFs. Shamshuddin *et al.,* [43] examined the flow of polymer-based THNFs with radiation and MHD effects. They found that thermal radiation parameters increase the energy transmission rate and enhance the heat transfer rate of trihybrid nanofluids. The THNFs (Cu, Fe_3O_4, SiO_2) exhibited higher velocity profiles compared to NFs (Cu) and HNFs (Cu-Fe_3O_4). A study of the ternary nanofluids considering the gyrotactic microorganisms with the effect of the activation energy, buoyancy forces and thermal radiation by Souayeh and Ramesh [44] found that the nanoparticle temperature of the ternary nanofluid enhances with the enhancement of activation energy and Brownian motion parameters. Meanwhile, the Brownian motion and radiation effects increase the microorganism profile.

Presently, the two mathematical models (homogeneous and non-homogeneous) are used to discuss the nanofluid transport. Homogeneous model, presented by Tiwari and Das [45] pointed out that enhanced thermophysical properties of base fluid are due to suspended nanoparticles. Buongiorno [46], who proposed the non-homogeneous model, identified seven possible factors which contribute to enhance heat transfer in nanofluid but mainly two of them, Brownian motion and thermophoresis were found to contribute significantly. This current research aims to explore the heat transfer rate within THNF flow over a vertical plate, considering various nanoparticle shapes and the presence of motile gyrotactic microorganisms with thermal radiation. The Buongiorno model treats the nanofluids' velocity as the sum of both the base fluid and relative velocities, emphasizing significant mechanisms like Brownian diffusion and thermophoresis. Conversely, the Tiwari Das model is employed to consider the solid volume fraction of the nanoparticle shapes. In this study, we utilize the Buongiorno model to account for Brownian motion and thermophoresis in the context of bioconvection flow, while the Tiwari Das model is utilized to analyse the volume fraction of the nanoparticles' shapes.

2. Mathematical Formulation

Consider a laminar, incompressible, steady, and two-dimensional boundary layer flow of THNF containing gyrotactic microorganisms over a vertical plate (see Figure 1).

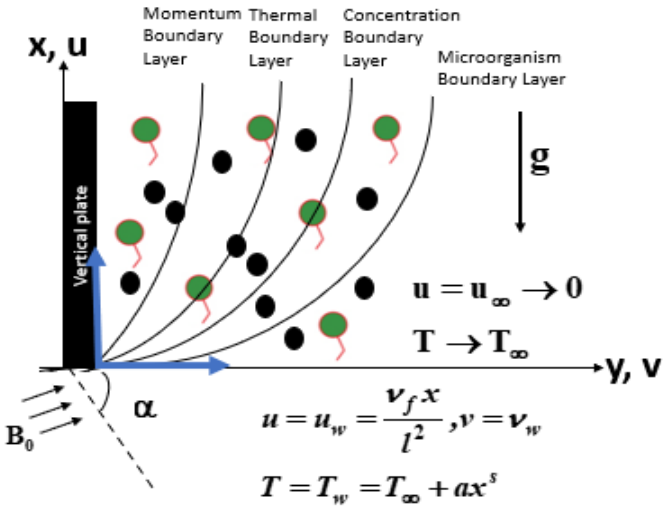

Fig. 1. Physical model for vertical plate

The microorganisms are usually found to flourish in natural water conditions. So, water is used as the base fluid and three different nanoparticles are chosen which are $\phi_{AI_2O_3}, \phi_{cu}$ and ϕ_{CNT} in this study. The aligned magnetic field with an acute angle, α is applied to the flow. It is recognized as a function of the distance from the origin expressed as $B(x) = B_0/\sqrt{x}$ with $B_0 \neq 0$. Under the assumption that a constant wall temperature boundary condition is imposed on the wall, we can derive the governing equations by employing scale analysis and implementing boundary layer approximations. These equations can be expressed as follows [23,37]:

$$\frac{\partial u}{\partial x} + \frac{\partial v}{\partial y} = 0 \tag{1}$$

$$u\frac{\partial u}{\partial x} + v\frac{\partial u}{\partial y} = \upsilon_{thnf}\left(\frac{\partial^2 u}{\partial y^2}\right) + \frac{(\rho\beta)_{thnf}}{\rho_{thnf}}\cos\alpha\left[g_T(T-T_\infty) + g_C(C-C_\infty) + g_N(N-N_\infty)\right] - \frac{\sigma B_0^2}{\rho_{thnf}}\sin^2\gamma(u) \tag{2}$$

$$(\rho C\rho)_{thnf}\left\{u\frac{\partial T}{\partial x} + v\frac{\partial T}{\partial y}\right\} = k_{thnf}\left(\frac{\partial^2 T}{\partial y^2}\right) + \tau\left[D_n\frac{\partial C}{\partial y}\frac{\partial T}{\partial y} + \frac{D_T}{T_\infty}\left(\frac{\partial T}{\partial y}\right)^2\right] + Q(T-T_\infty) - \frac{\partial qr}{\partial y} \tag{3}$$

$$u\frac{\partial C}{\partial x} + v\frac{\partial C}{\partial y} = \frac{D_T}{T_\infty}\frac{\partial^2 T}{\partial y^2} + D_n\frac{\partial^2 C}{\partial y^2} \tag{4}$$

$$u\frac{\partial N}{\partial x} + v\frac{\partial N}{\partial y} = D_m\frac{\partial^2 N}{\partial y^2} - \frac{1}{C_w - C_\infty}\frac{\partial}{\partial y}\left[N\frac{\partial C}{\partial y}\right]bW_c \tag{5}$$

where u is the fluid velocity and v is the normal velocity components along the x-axis and y-axis. T is the temperature, C is the concentration, N is motile microorganisms, , D_B is the Brownian diffusion coefficient, D_m is the diffusivity of microorganisms, D_T is the thermophoresis diffusion coefficient, Q is the heat source/sink coefficient, b is the chemotaxis constant, W_c is the maximum cell swimming speed (bW_c is assumed to be constant) and $\tau = (\rho c)_p/(\rho c)_f$ which is the ratio between the effective heat capacity of the nanoparticle material and the heat capacity of the base fluid with ρ_f being the density of the base fluid. The Rosseland approximation [28] gives the radiative heat flux term q_r of the form $q_r = \frac{4\sigma^*}{3k^*}\frac{\partial T^4}{\partial y}$. T^4 may be written as $T^4 = T_\infty^4\left[1 + (\theta_w - 1)\theta\right]^4$ where $\theta_w = T_w/T_\infty$ is the wall temperature excess ratio parameter.

The respective boundary conditions applied in this investigation are outlined below [28]:

$$\begin{aligned} &u = u_w = \frac{\nu_f x}{l^2},\ v = v_w,\ T = T_w = T_\infty + ax^s,\ C = C_w,\ N = N_w \quad at\ y = 0 \\ &u \to 0,\ T \to T_\infty,\ C \to C_\infty,\quad N \to N_\infty \quad as\ y \to \infty \end{aligned} \tag{6}$$

where T_w, C_w, and N_w are temperature, nanoparticle concentration and density of the motile microorganisms at the plate surface. The v_w as the velocity of mass transfer which corresponds to

$v_w > 0$ is suction and $v_w < 0$ is injection, and the surface is moving with initial velocity $u_w = \frac{v_f x}{l^2}$. The temperature at the surface T_w is taken as a variable $T_\infty + ax^s$, where T_∞ is the free stream temperature, and s is the parameter related to surface temperature. The thermophysical properties of the nanoparticle's attributes are provided in Table 1 along with the thermophysical relation of THNF as shown in Table 2.

Table 1
Thermophysical Properties of Base Fluid and Nanoparticles [23]

Properties	Base Fluid (Water)	Al_2O_3	Cu	CNT
$\rho(kg/m^3)$	997.1	3970	8933	2600
$C_p(J/kgK)$	4179	765	385	425
$k(W/mk)$	0.613	40	400	6600
$\beta \times 10^{-5}$	21	0.85	1.67	1.6x10^{-6}
Shape		Spherical	Platelet	Cylindrical
Sphericity		$\psi = 1$	$\psi = 0.612$	$\psi = 0.52$
Pr	6.2			

The thermophysical relation of THNF properties shown in Table 2**.** The $\phi_{AI_2O_3}, \phi_{cu}$ and ϕ_{CNT} represents the volume fractions of the first, second, and third types of nanoparticles respectively while THNF is the ternary hybrid nanofluids, HNF represents the hybrid nanofluids and NF denotes as the nanofluids.

Table 2
Thermophysical Relation of Ternary Hybrid Nanofluids [23]

Properties	Ternary Hybrid Nanofluids	
Density	$\mu_{thnf} = \left(1-\phi_{AI_2O_3}-\phi_{cu}-\phi_{CNT}\right)\rho_{bf} + \phi_{AI_2O_3}\rho_{sp1} + \phi_{cu}\rho_{sp2} + \phi_{CNT}\rho_{sp3}$	(7)
Heat Capacity	$\left(\rho C_p\right)_{thnf} = \left(1-\phi_{AI_2O_3}-\phi_{cu}-\phi_{CNT}\right)\left(\rho C_p\right)_{bf} + \phi_{AI_2O_3}\left(\rho C_p\right)_{sp1} + \phi_{cu}\left(\rho C_p\right)_{sp2} + \phi_{CNT}\left(\rho C_p\right)_{sp3}$	(8)
Thermal Expansion Coefficient	$\left(\rho\beta\right)_{thnf} = \left(1-\phi_{AI_2O_3}-\phi_{cu}-\phi_{CNT}\right)\left(\rho\beta\right)_{bf} + \phi_{AI_2O_3}\left(\rho\beta\right)_{sp1} + \phi_{cu}\left(\rho\beta\right)_{sp2} + \phi_{CNT}\left(\rho\beta\right)_{sp3}$	(9)
Modified Maxwell model	$\frac{k_{nf_i}}{k_{bf}} = \frac{k_i + (n-1)k_{bf} + (n-1)\phi_i\left(k_i - k_{bf}\right)}{k_i + (n-1)k_{bf} + \phi_i\left(k_i - k_{bf}\right)}$ where, $n = \left(\frac{3}{\psi}\right)$ is shape factor	(10)
Nanoparticles-2 spherical →	$\frac{\mu_{nf1}}{\mu_{bf}} = 1 + 2.5\phi_{AI_2O_3} + 6.2\phi_{AI_2O_3}{}^2$ $\frac{k_{nf1}}{k_{bf}} = \frac{k_1 + 2k_{bf} + 2\phi_{AI_2O_3}\left(k_1 - k_{bf}\right)}{k_1 + 2k_{bf} - \phi_{AI_2O_3}\left(k_1 - k_{bf}\right)}$	(11)
Nanoparticles-2 platelet →	$\frac{\mu_{nf2}}{\mu_{bf}} = 1 + 13.5\phi_{cu} + 904.4\phi_{cu}{}^2$ $\frac{k_{nf2}}{k_{bf}} = \frac{k_2 + 3.9k_{bf} + 3.9\phi_{cu}\left(k_2 - k_{bf}\right)}{k_2 + 3.9k_{bf} - \phi_{cu}\left(k_2 - k_{bf}\right)}$	

Nanoparticles-3	cylindrical →	$\frac{\mu_{nf3}}{\mu_{bf}} = 1 + 37.2\phi_{CNT} + 612.2\phi_{CNT}{}^2$ $\frac{k_{nf3}}{k_{bf}} = \frac{k_3 + 4.7k_{bf} + 4.7\phi_{CNT}\left(k_3 - k_{bf}\right)}{k_3 + 4.7k_{bf} - \phi_{CNT}\left(k_3 - k_{bf}\right)}$	
Viscosity		$\mu_{thnf} = \frac{\mu_{nf1}\phi_{AI_2O_3} + \mu_{nf2}\phi_{cu} + \mu_{nf3}\phi_{CNT}}{\phi_{thnf}}$	(12)
Thermal Conductivity		$k_{thnf} = \frac{k_{nf1}\phi_{AI_2O_3} + k_{nf2}\phi_{cu} + k_{nf3}\phi_{CNT}}{\phi_{thnf}}$ where $\phi_{thnf} = \phi_{AI_2O_3} + \phi_{cu} + \phi_{CNT}$	(13)

The mathematical formulation of the problem is simplified by introducing the following similarity variables (Eq. 15) to reduces the governing and boundary conditions to the ordinary differential equations (Eqs. 16-19) subjected to boundary conditions 20:

$$\eta = \frac{y}{l},\ u = \frac{\nu_f x}{l^2} f'(\eta),\ \ v = -\nu_f \frac{f(\eta)}{l}, \theta(\eta) = \frac{T - T_\infty}{T_w - T_\infty},\ \ \phi(\eta) = \frac{C - C_\infty}{C_w - C_\infty},\ \ \zeta = \frac{N - N_\infty}{N_w - N_\infty} \tag{15}$$

$$\frac{E1}{E2} f''' + f'^2 - (n+1) f f'' - M f' \sin^2\gamma + \frac{E3}{E2} Gr\left[Rb\zeta - Nr\phi - \theta\right]\cos\alpha \tag{16}$$

$$s f'\theta - (n+1) f\theta' = \frac{1}{E4}\left[\frac{1}{\mathrm{Pr}}(E5 + Rd)\theta'' + Nb\phi'\theta' + Nt\theta'^2 + Q\theta\right] \tag{17}$$

$$\phi'' + Lef\,\phi' + \frac{Nt}{Nb}\theta'' = 0 \tag{18}$$

$$\zeta'' + Lbf\,\zeta' - Pe\left[\phi''(\omega + \zeta) + \zeta'\phi'\right] = 0 \tag{19}$$

with the boundary conditions are as follows:

$$\begin{aligned} &f(0) = \frac{su}{n+1},\ \ f'(0) = 1,\ \ \theta(0) = 1,\ \ \phi(0) = 1,\ \ \zeta(0) = 1 \quad at\ y = 0 \\ &f'(\infty) = 0,\ \theta(\infty) = 0,\ \ \phi(\infty) = 0,\ \ \chi(\infty) = 0 \qquad at\ y \to \infty \end{aligned} \tag{20}$$

The parameters in Eqs. (16)-(19) are defined as:

$$E1 = \frac{\mu_{thnf}}{\mu_f},\ \ E2 = \frac{\rho_{thnf}}{\rho_f},\ \ E3 = \frac{(\rho\beta)_{thnf}}{(\rho\beta)_f},\ \ E4 = \frac{(\rho C_p)_{thnf}}{(\rho C_p)_f},\ \ E5 = \frac{k_{thnf}}{k_f},\ \ \mathrm{Re}_x{}^2 = \frac{u_w x}{\nu_f},\ \ u_w = \frac{\nu_f x}{l^2},$$

$$Gr = \frac{l^4(1 - C_\infty)\beta\rho_f(T_w - T_\infty)x^3}{\nu_f{}^2} = \frac{Gr_x}{\mathrm{Re}_x{}^2},\ Nr = \frac{(\rho_p - \rho_f)(C_w - C_\infty)}{(1 - C_\infty)\beta\rho_f(T_w - T_\infty)},\ \ Rb = \frac{(\rho_m - \rho_f)(N_w - N_\infty)}{(1 - C_\infty)\beta\rho_f(T_w - T_\infty)},$$

$$M=\frac{\sigma B_0^2 l^2}{\rho_{thnf}\nu_f},\ \mathrm{Pr}=\frac{\left(\rho C_p\right)_{thnf}\nu_f}{k_f},\ Rd=\frac{4\sigma^* T_\infty^3}{3k^* k_f},\ Nb=\frac{\left(\rho C_p\right)_p}{\left(\rho C_p\right)_f\nu_f}D_B\left(C_w-C_\infty\right),\ Nt=\frac{\left(\rho C_p\right)_p}{\left(\rho C_p\right)_f\nu_f}\frac{D_T\left(T_w-T_\infty\right)}{T_\infty}$$

$$Q=\frac{Ql^2}{\left(\rho C_p\right)_f\nu_f},Le=\frac{\nu_f}{D_B},\ Lb=\frac{\nu_f}{D_m},\ \ Pe=\frac{bW_c}{D_m},\ \ \omega=\frac{N_\infty}{\left(N_w-N_\infty\right)},\ Su=-\frac{-\upsilon_w l}{\nu_f}$$

where η is the similarity variable, $\nu_f=\mu_f/\rho_f$ is kinematic viscosity, Pr is the Prandtl number, M is the magnetic parameter number, Rd is thermal radiation parameter, Gr denotes the local Grashof number, Nr is the buoyancy ratio parameter, Rb is the bioconvection Rayleigh number, Nb is the Brownian motion parameter, Nt is the thermophoresis parameter, Le is the Lewis number, Lb is the bioconvection Lewis number, Pe is the bioconvection Peclet number, Q is heat source, ω is a dimensionless bioconvection constant and Su is the suction $\left(Su>0\right)$ / injection $\left(Su<0\right)$. The parameter s related to surface temperature. A solution will be viable exclusively when $s=1$ because it causes the x term to disappear. To ensure a corresponding solution exists and to facilitate the computation of results in this study, the parameter linked to surface temperature must be rigorously confined to $s=1$ [23]. The quantities of engineering interest in dimensionless form like skin friction coefficient c_f, the local Nusselt number Nu_x, the Sherwood number Sh_x and the Motile Microorganism number Nn_x defined as:

$$c_f=\frac{\tau_w}{\left(\mu u_w x/l^3\right)},\ \ Nu_x=-\frac{xq_w}{k_f\left(T_w-T_\infty\right)},\ Sh_x=\frac{-xq_m}{D_n\left(C_w-C_\infty\right)},\ Nn_x=\frac{-xq_n}{D_m\left(N_w-N_\infty\right)} \tag{21}$$

where ρ_f is the density of nanofluids, τ_w is the shear stress or wall skin friction, q_w is the surface heat flux, k_f is the thermal conductivity of the nanofluids, q_n is surface mass flux and q_m is the surface motile microorganisms' flux which is defined as;

$$\tau_w=\mu_{thnf}\left(\frac{\partial u}{\partial y}\right)_{y=0},\ \ q_w=\left(k_{thnf}\frac{\partial T}{\partial y}+\frac{4\sigma^*}{3k^*}\frac{\partial T^4}{\partial y}\right),\ \ q_m=D_B\left(\frac{\partial C}{\partial y}\right)_{y=0},\ \ \ q_n=D_m\left(\frac{\partial N}{\partial y}\right)_{y=0} \tag{22}$$

By using similarity variables, the non-dimensional skin friction coefficient, Nusselt number, Sherwood number are and Motile Microorganism number are obtained as:

$$\frac{c_f}{\mathrm{Re}_x^{\frac{1}{2}}}=E1f''(0),\ \ \frac{Nu_x}{\mathrm{Re}_x^{\frac{1}{2}}}=-\left(E5+\frac{4}{3}Rd\right)\theta'(0),\ \ \frac{Sh_x}{\mathrm{Re}_x^{\frac{1}{2}}}=-\phi'(0),\ \ \ \frac{Nn_x}{\mathrm{Re}_x^{\frac{1}{2}}}=-\zeta'(0)$$

3. Numerical Solution and Validation

To efficiently tackle the numerical solution of non-linear differential equations [Eq. (16)-(19)] alongside the boundary conditions specified in Eq. (20), we employed the bvp4c algorithm, which is readily available in MATLAB software. This algorithm utilizes a finite-difference method to execute the three stages of the Lobatto IIIa formula, originally introduced by Shampine *et al.,* [47]. The Lobatto IIIa method belongs to the family of Runge-Kutta methods and makes use of the implicit trapezoidal rule, closely associated with the collocation method. The bvp4c function is the

embodiment of the collocation technique. To begin, we first need to reduce Eq. (16)-(19) into first-order differential equations as follows:

$$y(1)=f,\ y(2)=f',\ y(3)=f'',\ y(4)=\theta,\ y(5)=\theta',\ y(6)=\phi,\ y(7)=\phi',\ y(8)=\zeta,\ y(9)=\zeta' \tag{23}$$

Subsequently, utilizing these newly introduced variables, we can express the system of Eq. (16)-(19) as follows:

$$\frac{dy(1)}{dn}=f'=y(2)$$
$$\frac{dy(2)}{dn}=f''=y(3)$$
$$\frac{dy(3)}{dn}=f'''=\frac{E1}{E2}\left(-y(2)^2-y(1)y(3)+My(2)\sin^2(\gamma)-\frac{E3}{E2}\left[G_T y(4)+G_C y(6)+G_N y(8)\right]\cos\alpha\right)$$
$$\frac{dy(4)}{dn}=\theta'=y(5)$$
$$\frac{dy(5)}{dn}=\theta''=\left(\frac{Q}{E4}y(4)+sy(2)y(4)-y(1)y(5)-Nby(7)y(5)-Nty(5)y(5)\right)/\frac{1}{E4\,\mathrm{Pr}}\left(E5+\frac{4}{3}Rd\right)$$
$$\frac{dy(6)}{dn}=\phi'=y(7)$$
$$\frac{dy(7)}{dn}=\phi''=-Ley(1)y(7)+\frac{Nt}{Nb}y(5)$$
$$\frac{dy(8)}{dn}=\zeta'=y(9)$$
$$\frac{dy(9)}{dn}=\zeta''=-Lby(9)y(1)+Pe\left(y(9)y(7)+y(7)\left(\omega+y(8)\right)\right)$$

In this model, we set $\eta_{\max}$ to a value of 6, as the conditions at this point were satisfied asymptotically, and step size was taken as 0.01. The values of slopes not known are guessed to begin the process of solving the equations. The iteration process is repeated, and the solution is acknowledged only when boundary condition is met. To affirm the precision and reliability of our current solution, we conducted a comparison between our results and those from [23], which are showcased in Table 3. The table reveals favorable comparative outcomes, instilling confidence in the methodology applied in this research.

Table 3
Comparison Results of c_f and Nu_x for Different Values of magnetic parameter $\gamma, \mathrm{Pr}, Gr, M, s$ when $Rd = Nb = Nt = Le = Lb = \omega = Q = S = 0$

γ	Pr	Gr	M	s	c_f		Nu_x	
					[23],[28]	Present	[23],[28]	Present
-5	0.3	-0.5	1	-2.1	-0.155302	-0.15530213	-2.236105	-2.23810511
-5	0.3	-0.5	1	2.1	-0.155705	-0.15570523	-2.232736	-2.23273621
-5	0.3	-0.5	3	2.1	-0.126332	-0.12633214	-2.233693	-2.23369331
-5	1.0	0.5	3	2.1	0.125683	0.12568332	-2.238416	-2.23841614
-5	1.0	0.5	3	2.1	0.125408	0.12540805	-2.243849	-2.24384922
1	1.0	0.5	3	2.1	0.353104	0.35310411	0.981690	0.98169001

4. Result and Discussion

The result describes the effects of the various parameters on THNF, HNF and NF over vertical plate parameters on different profiles which are velocity, temperature, concentration, and microorganisms' profiles by the graph while the skin friction, Nusselt number, Sherwood number and motile microorganism that are impacted by the parameters for THNF represent in table. To examine the effects of various parameters on different profiles, the values to the parameters assign as $\Pr = 6.2, M = 3, Rd = 2.5, Nb = 0.6, Nt = 0.7, Gr = 0.7, Nr = 0.3, Rb = 0.5, Q = 1.5, Lb = 2.5, Pe = 2, Le = 5,$ $Su = 0.2, \omega = 1.2$ and $s = 1(\text{fixed})$ in the NF (Al_2O_3-Water), HNF (Al_2O_3/Cu-Water) and THNF (Al_2O_3/Cu/CNT-Water) throughout the study.

4.1 Result and Discussion on Velocity Profile

Figures 2-11 shows the influence of the $\phi_{AI_2O_3}, \phi_{cu}$ and ϕ_{CNT} nanoparticles as notify as ϕ_1, ϕ_2 and ϕ_3 on the suction/injection parameter (Su), magnetic parameter (M), Grashoff number (Gr), bioconvection Rayleigh number (Rb), and buoyancy ratio parameter (Nr) respectively in the velocity profile. As seen in Figure 2 shows the increasing of $\text{NF}(\phi_{AI_2O_3})$ nanoparticles in the working fluid causes the velocity is decrease. The decrease in velocity due to an increase in $\text{NF}(\phi_{AI_2O_3})$ nanoparticles is due to the spherical shape since the spherical shape has a larger surface area for interacting with other shape of the nanoparticles. While, the $\text{HNF}(\phi_{cu})$ and $\text{THNF}(\phi_{CNT})$ nanoparticles in the working fluid causes the velocity is increase in Figures 3-4. Figure 5 displays that the velocity of NF is drops with an increasing value of the suction/injection parameter, Su. The application of suction/injection at the boundary layer is often used to delay the boundary layer separation. The increasing suction at the surface causes the thickness of the momentum boundary layer to reduce. The effect of the situation causes the layers of flow are strongly held toward the surface destruct the momentum, and hence, velocity decreases. The reverse effect is observed with a velocity increase in HNF and THNF. Figure 8 shows that the rising values of the magnetic field parameter M, decrease the velocity profile for NF, HNF, and THNF. A decreasing trend in Figure 8 is means that the flow is retarded by the increasing magnetic parameter and this result agrees with the expectations. As, the increase in value of M, also leads to increase the Lorentz force and it opposes the flow. Consequently, the decreasing trend in velocity is witnessed. Also, the momentum boundary layer thickness decreases with M. It is can be seen that velocity is higher for the flow in NF compared to HNF and THNF. The fluid to flow rapidly near the boundary layer is influenced by Grasshof number. In this study, the influence of Gr on the velocity show in Figure 9. An acceleration in the boundary layer flow will be observed for large values of Gr. Figure 9 show a rise in flow velocity, with an increase in Gr. The velocity profiles of the THNF over HNF and NF is increase with increase in the values of Gr. Moreover, from this figure that, the dimensionless velocity profile of THNF is higher than the velocity profile of HNF and NF. Figure 10 displays the variation values of bioconvection Rayleigh number, Rb on the velocity profile. The influence of bioconvection Rayleigh number Rb is more on the momentum equation since bioconvection plumes, buoyancy effect counteracts by the upward movement of the base fluid and nanoparticles. It is cause that increasing of value Rb is reduces the velocity of the fluid and the momentum boundary layer thickness as shown in the Figure 10. In the case of absence of bioconvection, parameter $Rb = 0$, the velocity at the plate is seen to be higher. The influence of the buoyancy ratio parameter, Nr on the velocity profile of bioconvection flow is presented in Figure 11. It is can be seen that the velocity profile decreases with variation values of Nr.

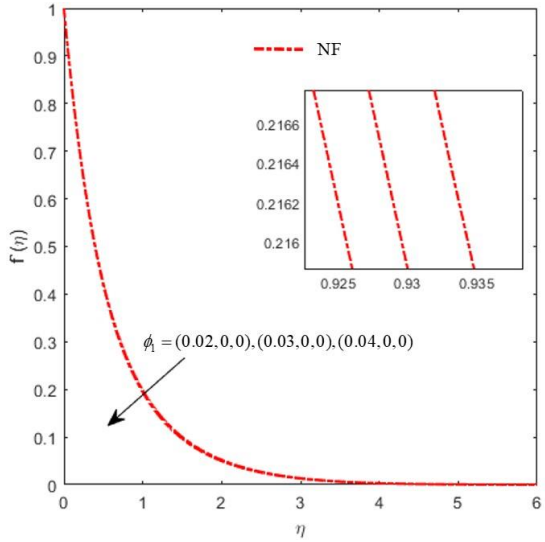

Fig. 2 Influence of $\phi_1(\mathrm{NF})$ on velocity profiles

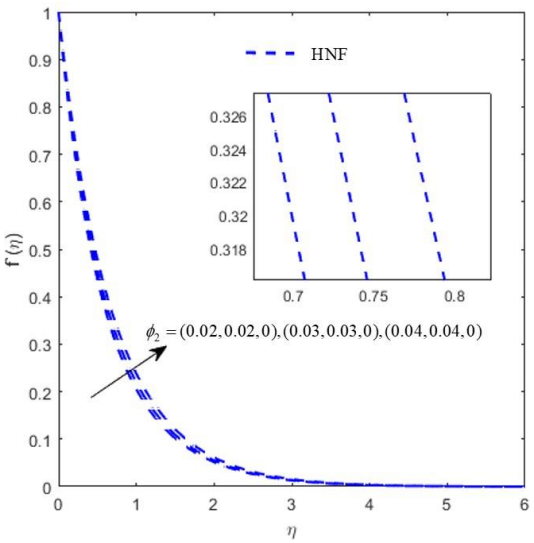

Fig. 3 Influence of $\phi_2(\mathrm{HNF})$ on velocity profiles

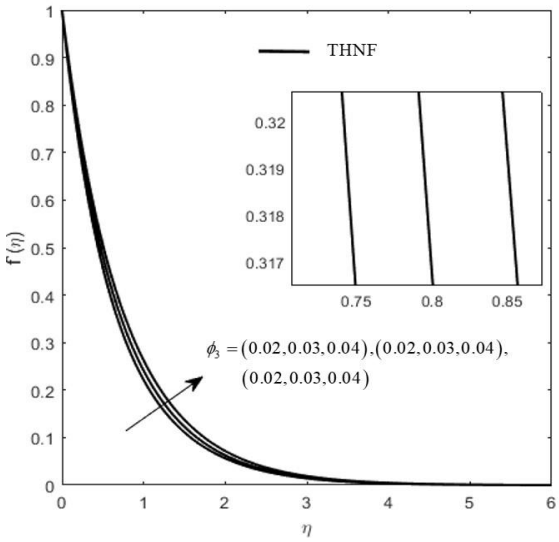

Fig. 4 Influence of $\phi_3(\mathrm{THNF})$ on velocity profiles

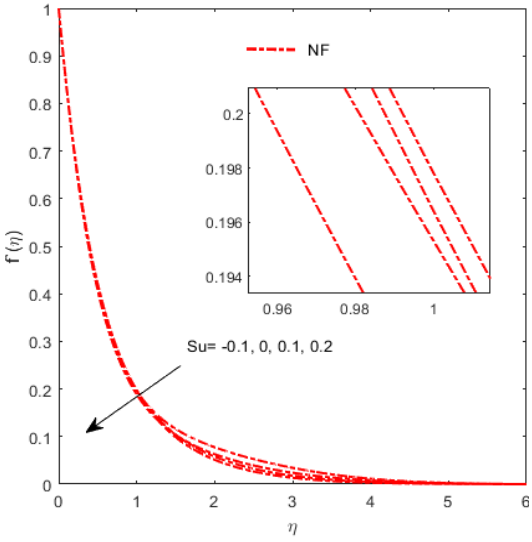

Fig. 5 Influence of $Su(\mathrm{NF})$ on velocity profiles

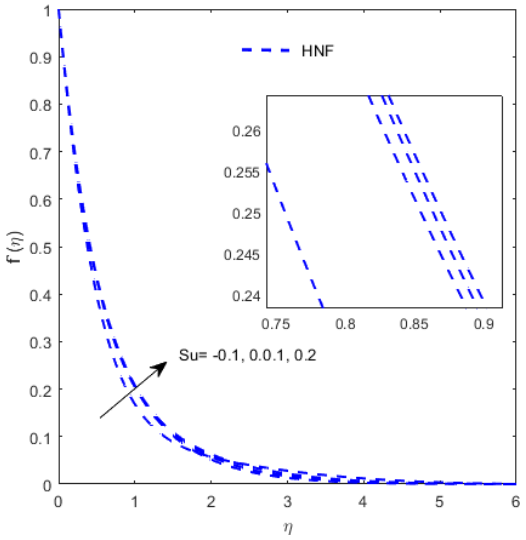

Fig. 6 Influence of $Su(\mathrm{HNF})$ on velocity profiles

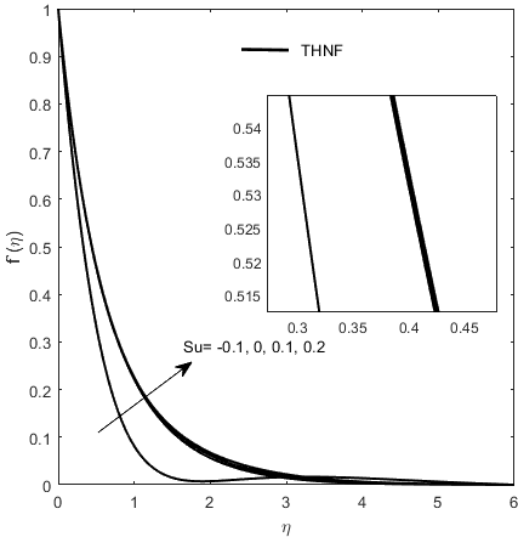

Fig. 7 Influence of $Su(\mathrm{THNF})$ on velocity profiles

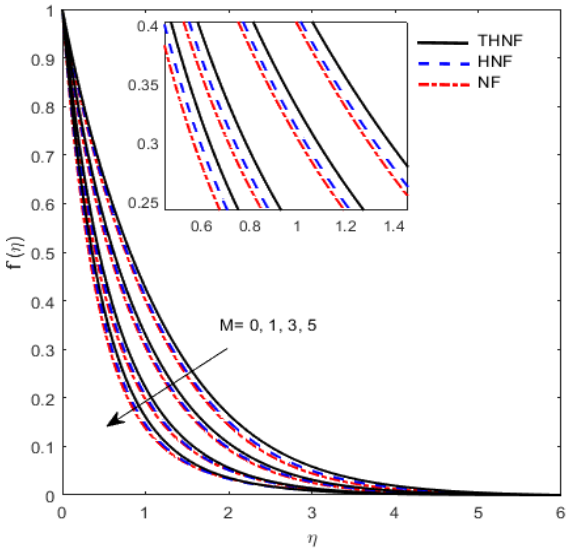

Fig. 8 Effects of M on velocity profiles

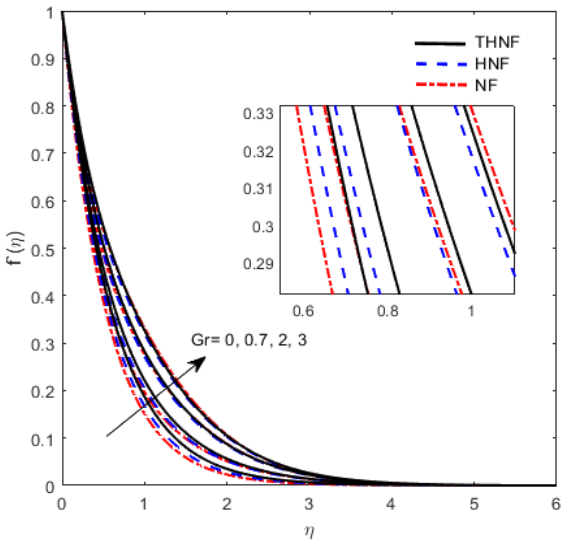

Fig. 9 Effects of Gr on velocity profiles

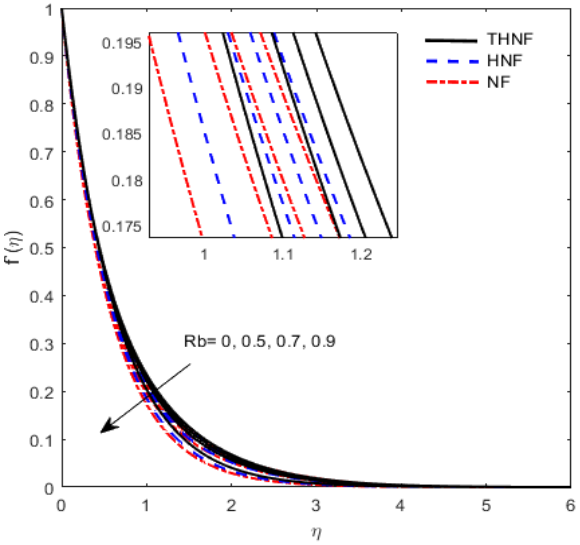

Fig. 10 Effects of Rb on velocity profiles

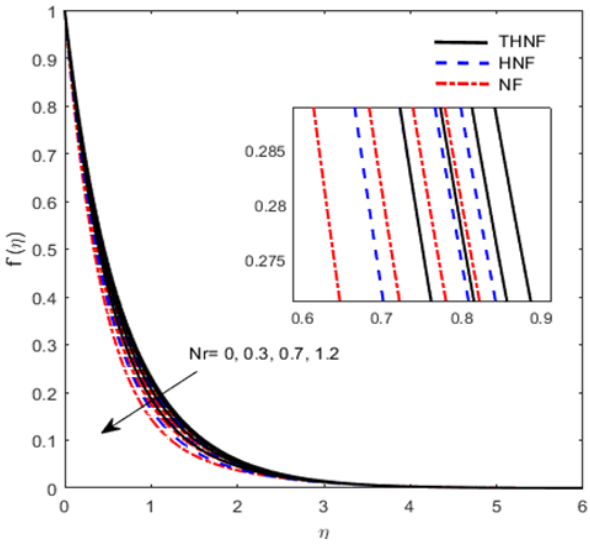

Fig. 11 Effects of Nr on velocity profiles

4.2 Result and Discussion on Temperature Profile

Figures 12-17 shows the influence of the $\phi_{AI_2O_3}, \phi_{cu}$ and ϕ_{CNT} nanoparticles as notify as ϕ_1, ϕ_2 and ϕ_3 on the suction/injection parameter (Su), Radiation parameter (Rd), Heat source parameter (Q), Thermophoresis effect (Nt), and Brownian motion parameter (Nb) respectively in the temperature profile. Figure 12 shown that an increase of $\phi_{AI_2O_3}, \phi_{cu}$ and ϕ_{CNT} nanoparticles in the working fluid cause the decrease in temperature in NF, HNF and THNF. The higher of the temperature in NF due to an increase in $\mathrm{NF}\left(\phi_{AI_2O_3}\right)$ nanoparticles because of the spherical shape since the spherical shape has a larger surface for interacting with other nanoparticles shape compared to the temperature in HNF and THNF. The lower of temperature in THNF due to spherical shape in $\mathrm{NF}\left(\phi_{AI_2O_3}\right)$ cause the viscosity of THNF increases and a greater amount of heat is released. Consequently, the temperature *in* THNF is decrease with an increment in the $\mathrm{NF}\left(\phi_{AI_2O_3}\right)$ nanoparticles. Figure 13 demonstrates the effect of the temperature profile due to fluctuating values of the suction/injection parameter, Su. The

increase in Su, the temperature is seen drop. When $Su<0$ for injection value is found higher in temperature compared to suction value $Su>0$. Figure 14 represent the impact of radiation parameter, Rd on temperature distribution. As the value of Rd increases, the temperature decreases, causing the thermal boundary layer to become thinner. Subsequently, layers within the flow having zero momentum receive energy, gain momentum, and restart their motion. This phenomenon disrupts the flow and diminishes friction at the boundary layer due to the presence of layers with zero momentum, resulting in a temperature drop. Consequently, the transfer of radiation heat to the fluid decreases, and the fluid temperature also declines. The term Nt, representing thermophoresis, is defined as the ratio of nanoparticle diffusion induced by the thermophoresis force to thermal diffusion in the fluid. According to Buongiorno, solid nanoparticles within the nanofluids experience a force opposing the imposed temperature gradient [48]. The selection of Nt values is aimed at simulating practical applications in areas such as heat exchangers, chemical engineering, porous media flows, and more. These values are based on the comprehensive research conducted by Buongiorno [46], a highly referenced study in the field of nanofluids convection. The Figure 15 shows the influence of Nt on temperatures is gradually diminishes. The nanoparticle volume fraction is affected by the Nt effect because the fluid's mass transfer rate is increased by Nt leading to a decreased rate of surface mass transfer. An increase in Nt, generates thermophoresis forces that facilitate the movement of nanoparticles from hotter regions to colder ones. Consequently, this leads to an expansion of the thermal boundary layer thickness. The interaction between nanoparticle and thermophoresis decreases the fluid viscosity, hence increasing its motion. The Brownian motion parameter, Nb, is a measure of the ratio between nanoparticle diffusion, driven by the Brownian motion effect, and nanofluid thermal diffusion. The intensity of Brownian motion depends on both particle size and the viscosity of the dispersion medium. Specifically, smaller particles and less viscous dispersion mediums result in more vigorous Brownian motion, and conversely, larger particles and more viscous mediums lead to less pronounced Brownian motion [49]. The Brownian motion parameter can be further described as the ratio of nanoparticle diffusion, attributed to Brownian motion, relative to nanofluid thermal diffusion. Consequently, an increase in the Brownian motion parameter is expected as the difference between nanoparticle volume fractions at the wall of the plate increases. In line with the Einstein-Stokes equation, Brownian motion is inversely proportional to particle diameter. Therefore, as particle diameter decreases, Brownian motion intensifies. Figure 16 display the effects of various Brownian motion parameters, Nb on the temperature profiles is decrease in the temperature of the fluid. The influence of heat source parameter, Q on temperature profile is shown in the Figure 17 increases the thermal conductivity and increases the fluids' temperature. Physically, an increase in the heat source parameter means an increase in the heat generated inside the boundary layer. In this study, the heat sink parameter $(Q<0)$ is not considered. It is observed that NF (Water- Al_2O_3) flow has a higher temperature compared to HNF (Water- Al_2O_3/Cu) and THNF (Water- Al_2O_3/Cu/CNT).

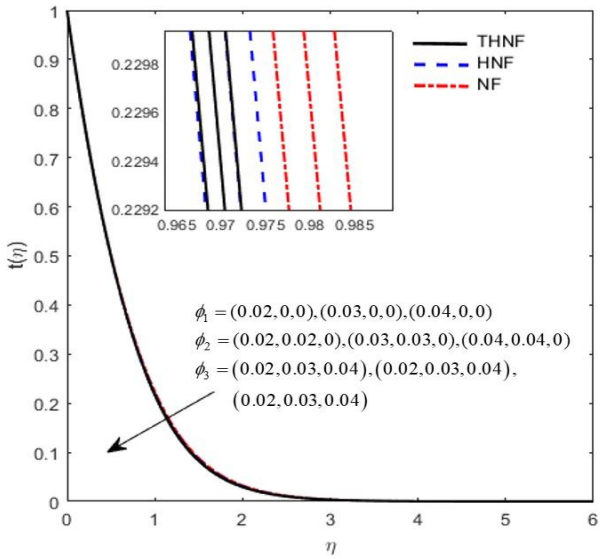

Fig. 12 Influence of ϕ on temperature profiles

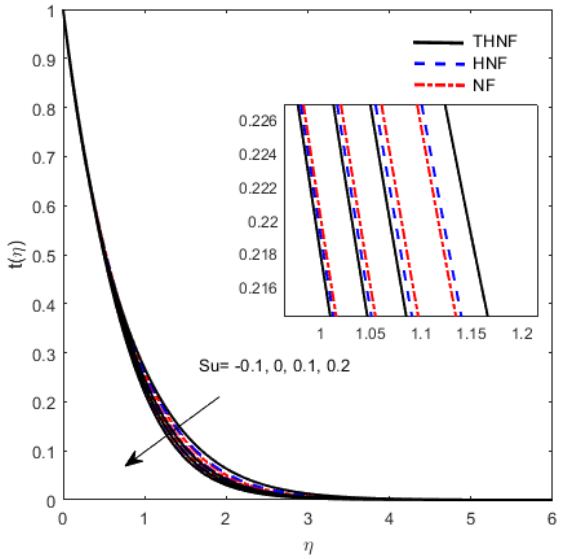

Fig. 13 Influence of Su on temperature profiles

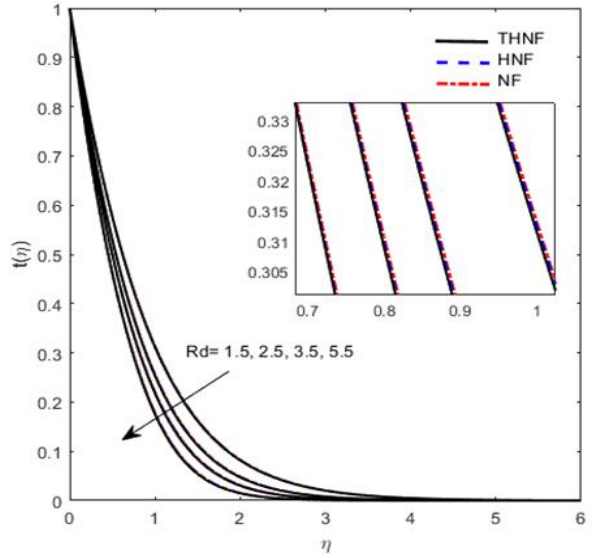

Fig. 14 Influence of Rd on temperature profiles

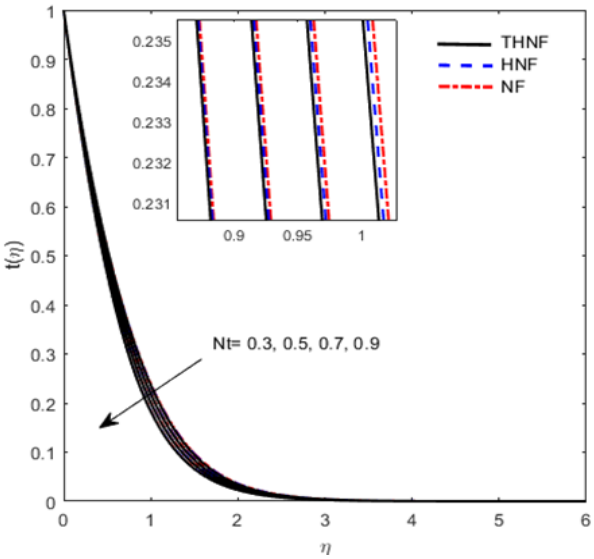

Fig. 15 Influence of Nt on temperature profiles

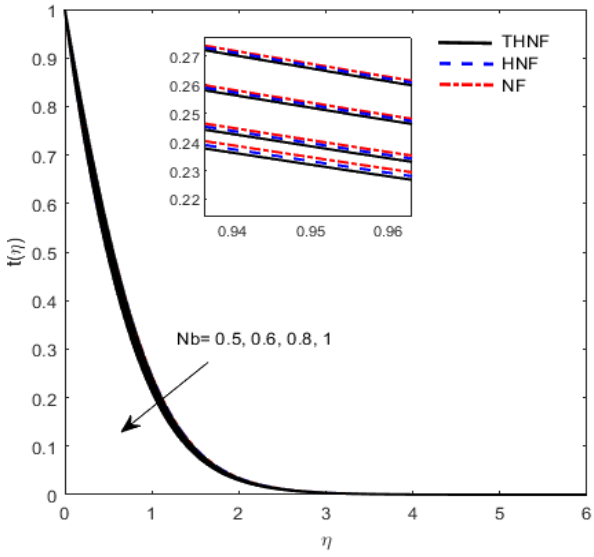

Fig. 16 Influence of Nb on temperature profiles

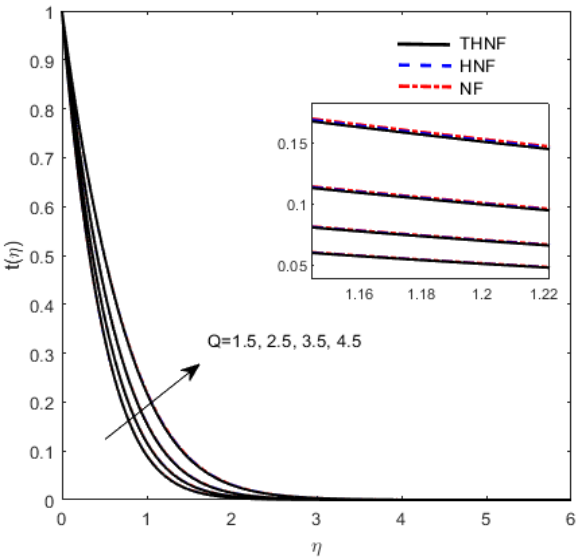

Fig. 17 Influence of Q on temperature profiles

4.3 Result and Discussion on Concentration Profile

Figures 18-22 shows the influence of the $\phi_{AI_2O_3}, \phi_{cu}$ and ϕ_{CNT} nanoparticles as notify as ϕ_1, ϕ_2 and ϕ_3 on the suction/injection parameter (Su), Lewis number (Le), Thermophoresis effect (Nt), and Brownian motion parameter (Nb) respectively in the concentration profile. The increasing of $\phi_{AI_2O_3}, \phi_{cu}$ and ϕ_{CNT} $\phi_{AI_2O_3}$ nanoparticles in the working fluid causes the concentration in Figure 18 is increases. Figure 19 displays that the concentration profile due to the suction/injection parameter, Su. When the Su at the surface gain the flow and momentum, enhance the diffusivity of the nanoparticles causes the concentration is rise due to the stronger suction. Figure 20 shows the decrease in the concentration of the profile with an increase in the Lewis number. The increase in Lewis number is seen as lower molecular diffusivity. The lower diffusivity of the nanoparticles in the boundary layer causes a decrease in concentration. In Figure 21, the thermophoresis value, Nt is increasing show that the concentration is decrease within the boundary layer. The increasing Brownian motion parameter, Nb in Figure 22, the concentration boundary layer thickness is increases. Hence, concentration increases within the boundary layer. It is shown that THNF (Water-Al_2O_3/Cu/CNT) flow has a higher concentration compared to HNF (Water- Al_2O_3/Cu) and NF (Water-Al_2O_3).

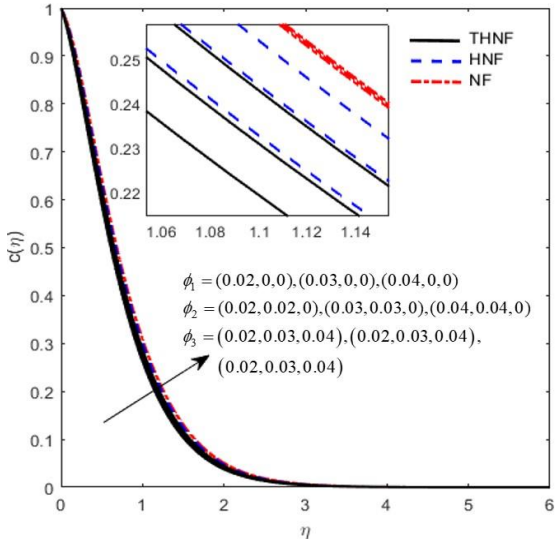

Fig. 18 Influence of ϕ on concentration profiles

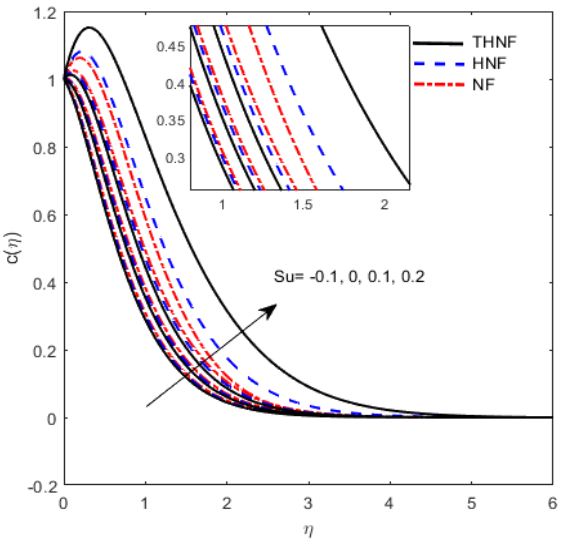

Fig. 19 Influence of Su concentration profiles

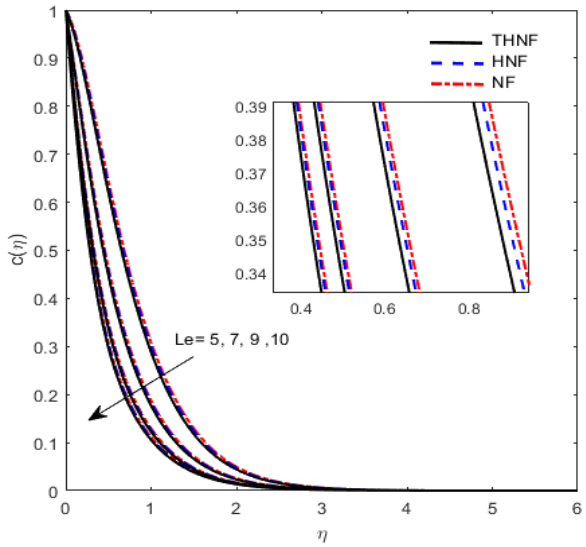

Fig. 20 Influence of Le concentration profiles

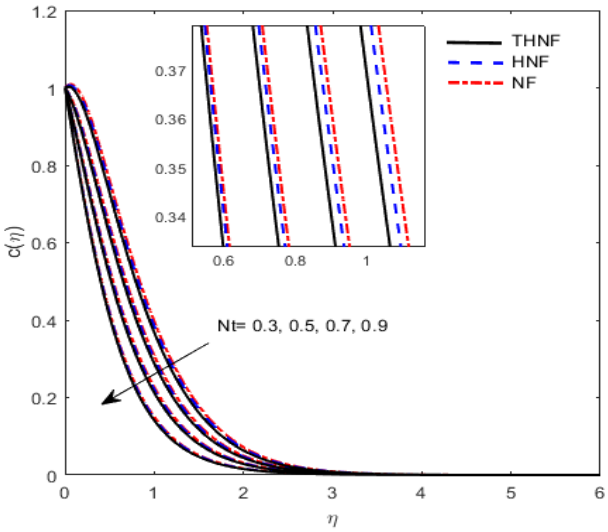

Fig. 21 Influence of Nt concentration profiles

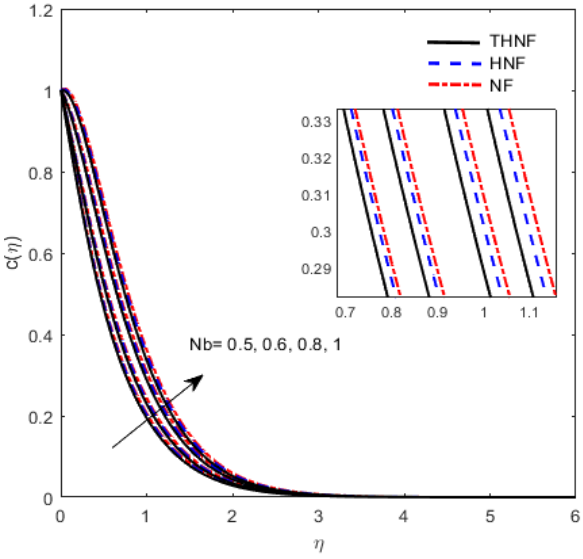

Fig. 22 Influence of Nb concentration profiles

4.4 Result and Discussion on Microorganisms Profile

Figures 23-27 shows the influence of the $\phi_{AI_2O_3}, \phi_{cu}$ and ϕ_{CNT} nanoparticles as notify as ϕ_1, ϕ_2 and ϕ_3 on the suction/injection parameter (Su), bioconvection Lewis number (Lb), bioconvection Peclet number (Pe), and dimensionless bioconvection constant (ω) respectively in the microorganisms profile. The increasing of $\phi_{AI_2O_3}, \phi_{cu}$ and ϕ_{CNT} $\phi_{AI_2O_3}$ nanoparticles in the working fluid causes the microorganisms profile in Figure 23 is increases in the working fluid causes the microorganism profile is increase. There is an exists the inflection point in microorganism's profile where $n > 1.1$ shows an increasing of $\phi_{AI_2O_3}, \phi_{cu}$ and ϕ_{CNT} nanoparticles in the working fluid causes the microorganism profile is decrease. Figure 24 shows that a rise in the suction/injection parameter, Su causes the microorganism profile to increase. A stronger effect of the suction/injection parameter increase the width of momentum and the boundary layer. As a result, the movement of layers and particles increase, and causes the increasing in the movement of the microorganism. The bioconvection Lewis number Lb is important in the bioconvection system to increases heat diffusivity at the surface and

lower the density of microbes. It also diminishes the width of the boundary layer, which is proportional to the density of the motile microbe. The influence of bioconvection Lewis number, Lb microorganisms' profiles in Figure 25 shows an increasing the value of Lb, the microorganism profile seen to increase. The different value of the bioconvection Peclet number, Pe shown in Figure 26 indicates that an improvement in the Pe leads to a rapid reduction in the thickness of motile microorganisms. It is observed in Figure 27 that the motile microorganisms rise with the increment in the Lewis number, Le but there is inflection point at $n>1.3$ that shows the opposite trend in the working fluid. The influence of the dimensionless bioconvection constant, ω show that an increment value of ω,the motile microorganism's profile is decrease. It is shown that THNF (Water-Al_2O_3/Cu/CNT) flow has a higher microorganisms density compared to HNF (Water- Al_2O_3/Cu) and NF (Water- Al_2O_3).

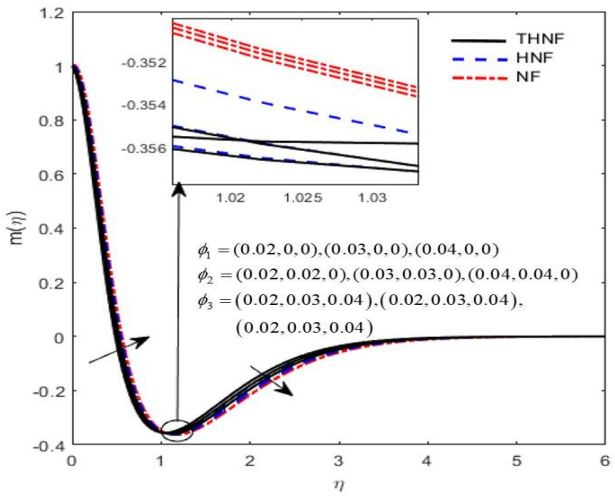

Fig. 23 Influence of ϕ microorganisms' profiles

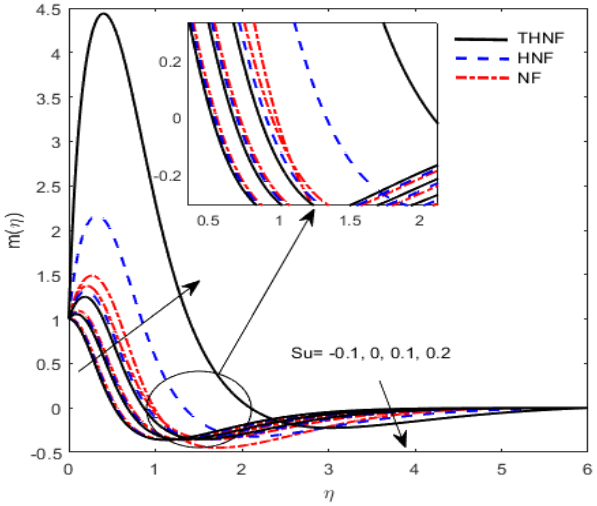

Fig. 24 Influence of Su microorganisms' profiles

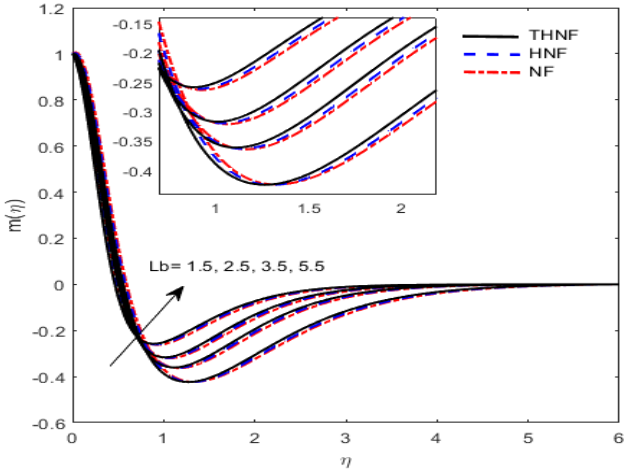

Fig. 25 Influence of Lb microorganisms' profiles

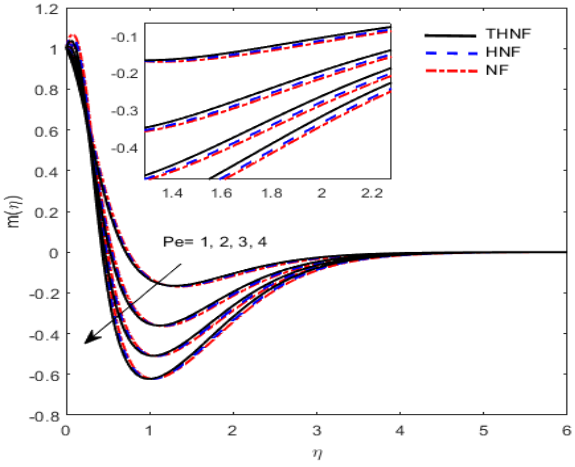

Fig. 26 Influence of Pe microorganisms' profiles

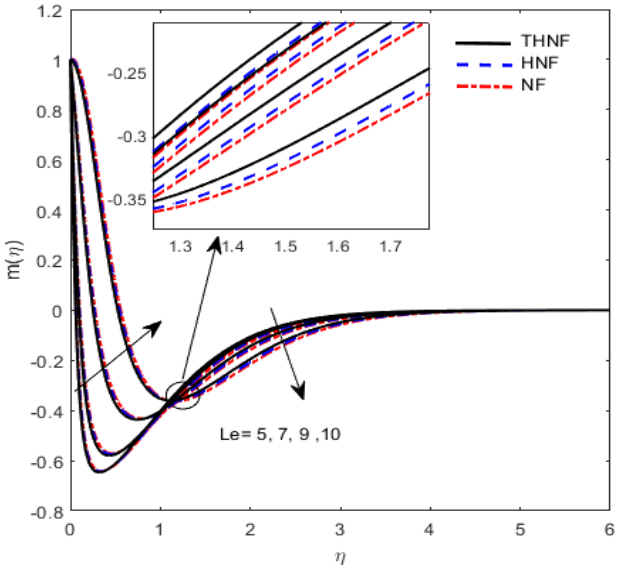

Fig. 27 Influence of Le microorganisms' profiles

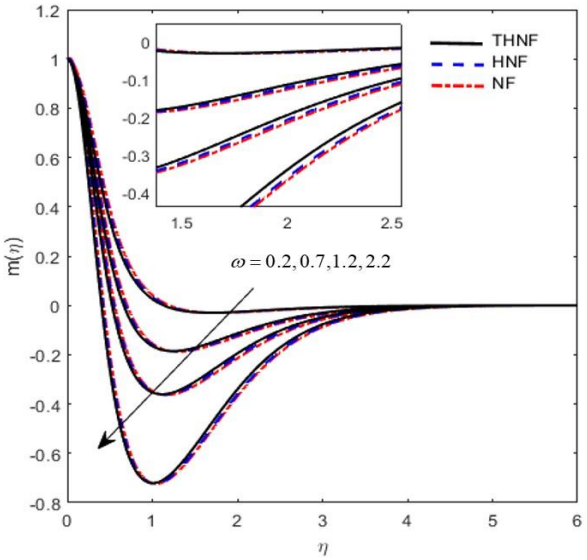

Fig. 28 Influence of ω microorganisms' profiles

Table 4 is shown that a higher density of spherical nanoparticles shape can lower the skin friction between the layers of water-based THNF. The increasing of $\phi_{Al_2O_3}$, ϕ_{cu} and ϕ_{CNT} for HNF and THNF nanoparticles shows the heat transfer is rising but on the other hand, an increase of $\phi_{Al_2O_3}$ for NF nanoparticles show that the heat transfer is decreased. The thermal boundary layer thickness reduces due to the increment of ϕ_{cu} and ϕ_{CNT} nanoparticles while thermal boundary layer thickness increases as the $\phi_{Al_2O_3}$ nanoparticles are increased. The decrease in the thermal boundary layer thickness leads to an increased heat transfer through the surface, resulting in an enhanced heat transfer rate. It shows the THNF (Water- Al_2O_3/Cu/CNT) is higher compared to HNF (Water- Al_2O_3/Cu) and NF (Water- Al_2O_3) in skin friction. It can be concluded that the THNF (Al_2O_3/Ag/Cu-Water) has a dense of viscosity of the fluid through which it passes. Whereas, the higher of the heat transfer is HNF (Water- Al_2O_3/Cu) compared to THNF (Water- Al_2O_3/Cu/CNT) and NF (Water- Al_2O_3).

Table 4
Result of Skin Friction, Nusselt Number, Sherwood Number, and Density Motile Microorganisms for Nanoparticles of NF, HNF, and THNF when $M=3, Rd=2.5, Nb=0.6, Nt=0.7, Gr=0.7, Nr=0.3, Rb=0.5, Le=5, Lb=2.5, Pe=2, \gamma=45, Su=0.2, \alpha=0, Q=1, \omega=1.5, s=1$(fixed)

$\phi_{Al_2O_3}$	ϕ_{cu}	ϕ_{CNT}	Skin Friction	Nusselt number	Sherwood number	Motile Microorganisms	
0.02	0	0	1.903728	5.854812	0.274726	-0.262320	
0.03	0	0	1.958283	5.876035	0.281453	-0.229752	Water- Al_2O_3
0.04	0	0	2.013865	5.897553	0.288805	-0.195335	
0.02	0.02	0	2.310235	5.861852	0.312258	-0.140357	
0.03	0.03	0	2.671609	5.881722	0.365627	0.031540	Water- Al_2O_3/Cu
0.04	0.04	0	3.093374	5.901415	0.424235	0.216655	
0.02	0.02	0.02	2.513051	5.834210	0.374236	0.061834	
0.03	0.03	0.03	2.976508	5.842713	0.443950	0.291249	Water- Al_2O_3/Cu/CNT
0.04	0.04	0.04	3.498906	5.852178	0.512281	0.518056	

Table 5 shows the skin friction, Nusselt number, Sherwood number, and density motile microorganisms for varies of parameter for THNF. An increment value in M, Nr, Rb, Nt, Q, and Su shows that the skin friction, Sherwood number, and motile microorganisms' density gradient is

decreased. Meanwhile Nr, Rb and Su show the opposite trend in both motile microorganisms' density gradient. The effect of $Gr, Nb, Le, Pe, Lb,$ and ω show that the skin friction, Sherwood number and motile microorganism's local density number is increase but a reverse trend is seen in the Nusselt number. The increasing value of the suction/injection parameters Su and Q causes an increase in the heat transfer rate. The increase in the heat transfer rate is due to a decrease in the thermal boundary layer thickness. On the contrary, the increasing suction parameter, Su causes the density gradient of the microorganisms to increase, while the increasing, Q parameter causes the density gradient of the microorganisms to decrease. An increasing value of Rd increase the value of skin friction, Nusselt number, Sherwood number, and density motile microorganisms. It means that a higher values for the Rd increase the heat transfer rate. This means that the radiation adds energy to the particles, which stimulates their movement and thus interaction with other particles, increasing the heat transfer rate. A rise in Nb enhances the motile microorganism's local density number. This may be attributed to the fact that at high Nb, there is a low concentration of nanoparticles., due to the higher plate surface concentration than in the fluid causing mass transfer to the fluid from the plate [48]. The accumulation of nanoparticles that form water-based THNF is a decreasing property of Nb due to the associated increasing random motion of nanoparticles in $\phi_{Al_2O_3}$ (spherical), ϕ_{cu} (platelet) and ϕ_{CNT} (cylindrical). The effect of thermophoresis, Nt and Brownian motion parameters, Nb on the local Sherwood number is quite contrary to each other. It is interesting to mention that Nb shows more impact on the mass transfer rate on the flow over a plate for THNF [50]. A rise in Nb and Pe increases the motile microorganism's local density number. This may be attributed to the fact that at high Pe, there is a low concentration of nanoparticles, due to the higher plate surface concentration than in the fluid causing mass transfer to the fluid from the plate [51]. A higher value of the Lewis number, Le and bioconvection Lewis number, Lb leads to maximizing the the motile microorganism's local density number which there is a substantial suppression in thermophoresis parameter, Nt. An increment of value of Lb boast the heat transfer but decrease in Le while skin friction and Sherwood number is increase but opposite trend in Lb.

Table 5
Result of Skin Friction (Sf), Nusselt Number (Nn), Sherwood Number (Sh), and Density Motile Microorganisms (Mn) for varies of parameter for THNF when $\phi_{Al_2O_3} = 0.02, \phi_{cu} = 0.02, \phi_{CNT} = 0.02$ is fixed

M	Rd	Gr	Nr	Rb	Nb	Nt	Le	Pe	Lb	Q	Su	ω	Sf (-)	Nn	Sh	Mn
0													1.3576	5.7818	0.7218	1.0732
1													1.8177	5.7987	0.5838	0.6572
3	2.5	0.7	0.3	0.5	0.6	0.7	5	2	2.5	1.5	0.2	1.2	2.5131	5.8342	0.3742	0.0618
5													3.0566	5.8679	0.2141	-0.4022
	1.5												2.5558	4.6159	-0.0351	-1.7452
	2.5												2.5131	5.8342	0.3742	0.0618
3	3.5	0.7	0.3	0.5	0.6	0.7	5	2	2.5	1.5	0.2	1.2	2.4841	6.9394	0.6158	1.1070
	5.5												2.4434	8.8719	0.9062	2.6503
		0											2.6140	5.8554	0.3106	-0.1106
		0.7											2.5131	5.8342	0.3742	0.0618
3	2.5	2	0.3	0.5	0.6	0.7	5	2	2.5	1.5	0.2	1.2	2.3114	5.8063	0.4778	0.3461
		3											2.1465	5.7918	0.5479	0.5439
			0										2.4333	5.8298	0.3985	0.1306
			0.3										2.5131	5.8342	0.3742	0.0618
3	2.5	0.7	0.7	0.5	0.6	0.7	5	2	2.5	1.5	0.2	1.2	2.6220	5.8412	0.3394	-0.0371
			1.2										2.7630	5.8522	0.2909	-0.1757
				0									2.4668	5.8465	0.3541	0.0135
3	2.5	0.7	0.3	0.5	0.6	0.7	5	2	2.5	1.5	0.2	1.2	2.5131	5.8342	0.3742	0.0618

				0.7									2.5314	5.8297	0.3817	0.0798
				0.9									2.5497	5.8253	0.3889	0.0972
					0.5								2.5541	6.1478	-0.0736	-1.7863
3	2.5	0.7	0.3	0.5	0.6	0.7	5	2	2.5	1.5	0.2	1.2	2.5131	5.8342	0.3742	0.0618
					0.8								2.4610	5.2586	0.9201	2.5174
					1.0								2.4262	4.7467	1.2368	4.8453
						0.3							2.4297	6.0959	1.4246	6.2258
3	2.5	0.7	0.3	0.5	0.6	0.5	5	2	2.5	1.5	0.2	1.2	2.4723	5.9492	0.9046	2.2607
						0.7							2.5131	5.8342	0.3742	0.0618
						0.9							2.5571	5.7485	-0.1735	-2.1984
							5						2.5131	5.8342	0.3742	0.0618
3	2.5	0.7	0.3	0.5	0.6	0.7	7	2	2.5	1.5	0.2	1.2	2.4360	5.4007	1.2027	3.9411
							9						2.3732	5.1036	1.9272	14.5376
							10						2.3510	4.9860	2.2627	24.7530
								1					2.5376	5.8414	0.3537	0.7467
3	2.5	0.7	0.3	0.5	0.6	0.7	5	2	2.5	1.5	0.2	1.2	2.5131	5.8342	0.3742	0.0618
								3					2.4967	5.8292	0.3885	-0.6336
								4					2.4854	5.8256	0.3990	-1.2807
									1.5				2.5123	5.8309	0.3805	-0.1258
3	2.5	0.7	0.3	0.5	0.6	0.7	5	2	2.5	1.5	0.2	1.2	2.5131	5.8342	0.3742	0.0618
									3.5				2.5127	5.8363	0.3704	0.2557
									5.5				2.5106	5.8389	0.3660	0.6571
										1.5			2.5131	5.8342	0.3742	0.0618
3	2.5	0.7	0.3	0.5	0.6	0.7	5	2	2.5	2.5	0.2	1.2	2.5456	7.1063	0.1873	-0.8753
										3.5			2.5725	8.2229	-0.0052	-1.8884
										4.4			2.5961	9.2344	-0.1951	-3.1046
											-0.1		6.3274	-1.0595	-28.996	6.3274
3	2.5	0.7	0.3	0.5	0.6	0.7	5	2	2.5	1.5	0	1.2	5.9310	-0.3050	-3.0899	5.9310
											0.1		5.8731	0.0247	-1.3016	5.8731
											0.2		5.8342	0.3742	0.0618	5.8342
												0.2	5.8473	0.3366	0.2209	5.8473
3	2.5	0.7	0.3	0.5	0.6	0.7	5	2	2.5	1.5	0.2	0.7	5.8405	0.3560	0.1322	5.8405
												1.2	5.8342	0.3742	0.0618	5.8342
												2.2	5.8233	0.4081	-0.0290	5.8233

5. Conclusions

In this research, the behavior of water-based NF, HNF and THNF carrying different nanoparticles shape is explored. This study involved the effects of MHD and radiation on velocity, temperature, concentration, microorganism distribution, local skin friction, heat transfer, Sherwood number, and microorganism density. Based on the discerned outcomes and observed results, we draw the following significant conclusions:

1. The increment of $\phi_{Al_2O_3}, \phi_{cu}$ and ϕ_{CNT} and Su shows that the velocity in NF is decrease but increase in HNF and THNF due to affect the different nanoparticles shape. Whereas, increase in both concentration and microorganism profile but decrease in temperature.
2. The velocity is decrease in the effect of M, Gr, Nr, Rb, Nt and Q but increase in temperature accept in Rb and Nt
3. The effect of $Rd, Gr, Nb, Lb, Le, Pe,$ and ω upsurge the velocity but reduce in temperature accept of Lb and Le
4. The concentration and microorganism profile are decrease due to $M, Nr, Nt, Nb,$ and Q but both increase in Rd, Gr, Rb, Pe and ω

5. The skin friction, Sherwood number, and density microorganism significantly are rise due to effect of $Rd, Gr, Nb,$ and Le.
6. The skin friction, Sherwood number, and density microorganism significantly are decrease due to effect of $M, Nr, Nt,$ and Q.
7. Rising values of Su was lessen the skin friction and rise the Nusselt number, Sherwood number, and density microorganism.
8. The motile density microorganism significantly increases with the influence of $Rd, Nr, Rb, Nb, Le, Lb,$ and Su.
9. The concentration and density microorganism of THNF is increase with higher value in Rd and M but decrease in velocity and temperature.
10. The skin friction between the boundary layers of water-based THNF is the lowest compared to NF and HNF, primarily because spherical nanoparticles exhibit greater density whereas the HNF has a higher Nussel number. Meanwhile, THNF has a higher Sherwood number and density microorganism compared to HNF and NF.

Acknowledgement
The authors extend their appreciation to Universiti Teknologi MARA for funding this work through MYRA Research Grant under grant number 600-RMC 5/3/GPM (026/2022).

References

[1] H. Adun, D. Kavaz, M. Dagbasi, Review of ternary hybrid nanofluid: synthesis, stability, thermophysical properties, heat transfer applications, and environmental effects, J. Clean. Prod. 328 (2021) 129525, https://doi.org/10.1016/j.jclepro.2021.129525

[2] Kandasamy, R., Nur Atikah Adnan, and Radiah Mohammad. "Nanoparticle shape effects on squeezed MHD flow of water-based Cu, Al_2O_3 and SWCNTs over a porous sensor surface." *Alexandria engineering journal* 57, no. 3 (2018): 1433-1445. https://doi.org/10.1016/j.aej.2017.03.011

[3] Rawi, Noraihan Afiqah, Mohd Rijal Ilias, Zaiton Mat Isa, and Sharidan Shafie. "Effect of Gravity Modulation on Mixed Convection Flow of Second Grade Fluid with Different Shapes of Nanoparticles." *Malaysian Journal of Fundamental and Applied Sciences* 13, no. 2 (2017). http://doi.10.11113/mjfas.v13n2.643

[4] Timofeeva, Elena V., Jules L. Routbort, and Dileep Singh. "Particle shape effects on thermophysical properties of alumina nanofluids." *Journal of applied physics* 106, no. 1 (2009). https://doi.org/10.1063/1.3155999

[5] Abbasi, M., M. M. Heyhat, and A. Rajabpour. "Study of the effects of particle shape and base fluid type on density of nanofluids using ternary mixture formula: A molecular dynamics simulation." *Journal of Molecular Liquids* 305 (2020): 112831. https://doi.org/10.1016/j.molliq.2020.112831

[6] Sahoo, Rashmi Rekha. "Thermo-hydraulic characteristics of radiator with various shape nanoparticle-based ternary hybrid nanofluid." *Powder technology* 370 (2020): 19-28. https://doi.org/10.1016/j.powtec.2020.05.013

[7] Manjunatha, S., V. Puneeth, B. J. Gireesha, and Ali Chamkha. "Theoretical study of convective heat transfer in ternary nanofluid flowing past a stretching sheet." *Journal of Applied and Computational Mechanics* 8, no. 4 (2022): 1279-1286.

[8] Ramzan, Muhammad, Farhan Ali, Nevzat Akkurt, Anwar Saeed, Poom Kumam, and Ahmed M. Galal. "Computational assessment of Carreau ternary hybrid nanofluid influenced by MHD flow for entropy generation." *Journal of Magnetism and Magnetic Materials* 567 (2023): 170353. https://doi.org/10.1016/j.jmmm.2023.170353

[9] Adun, Humphrey, Doga Kavaz, and Mustafa Dagbasi. "Review of ternary hybrid nanofluid: Synthesis, stability, thermophysical properties, heat transfer applications, and environmental effects." *Journal of Cleaner Production* 328 (2021): 129525. https://doi.org/10.1016/j.jclepro.2021.129525

[10] Sahoo, Rashmi Rekha, and Vikash Kumar. "Development of a new correlation to determine the viscosity of ternary hybrid nanofluid." *International Communications in Heat and Mass Transfer* 111 (2020): 104451. https://doi.org/10.1016/j.icheatmasstransfer.2019.104451

[11] Sahoo, Rashmi Rekha. "Thermo-hydraulic characteristics of radiator with various shape nanoparticle-based ternary hybrid nanofluid." *Powder technology* 370 (2020): 19-28. https://doi.org/10.1016/j.powtec.2020.05.013

[12] Animasaun, I. L., Se-Jin Yook, Taseer Muhammad, and Alphonsa Mathew. "Dynamics of ternary-hybrid nanofluid subject to magnetic flux density and heat source or sink on a convectively heated surface." *Surfaces and Interfaces* 28 (2022): 101654. https://doi.org/10.1016/j.surfin.2021.101654

[13] Raju, C. S. K., N. Ameer Ahammad, Kiran Sajjan, Nehad Ali Shah, Se-Jin Yook, and M. Dinesh Kumar. "Nonlinear movements of axisymmetric ternary hybrid nanofluids in a thermally radiated expanding or contracting permeable Darcy Walls with different shapes and densities: Simple linear regression." *International Communications in Heat and Mass Transfer* 135 (2022): 106110. https://doi.org/10.1016/j.icheatmasstransfer.2022.106110

[14] Shanmugapriya, M., R. Sundareswaran, P. Senthil Kumar, and Gayathri Rangasamy. "Impact of nanoparticle shape in enhancing heat transfer of magnetized ternary hybrid nanofluid." *Sustainable Energy Technologies and Assessments* 53 (2022): 102700. https://doi.org/10.1016/j.seta.2022.102700

[15] Elnaqeeb, Thanaa, Isaac Lare Animasaun, and Nehad Ali Shah. "Ternary-hybrid nanofluids: significance of suction and dual-stretching on three-dimensional flow of water conveying nanoparticles with various shapes and densities." *Zeitschrift für Naturforschung A* 76, no. 3 (2021): 231-243. https://doi.org/10.1515/zna-2020-0317

[16] Bosli, Fazillah, Alia Syafiqa Suhaimi, Siti Shuhada Ishak, Mohd Rijal Ilias, Amirah Hazwani Abdul Rahim, and Anis Mardiana Ahmad. "Investigation of Nanoparticles Shape Effects on Aligned MHD Casson Nanofluid Flow and Heat Transfer with Convective Boundary Condition." *Journal of Advanced Research in Fluid Mechanics and Thermal Sciences* 91, no. 1 (2022): 155-171. https://doi.org/10.37934/arfmts.91.1.155171

[17] Bosli, Fazillah, Mohd Rijal Ilias, Noor Hafizah Zainal Aznam, Siti Shuhada Ishak, Shahida Farhan Zakaria, and Amirah Hazwani Abdul Rahim. "Aligned magnetohydrodynamic effect on magnetic nanoparticle with different base fluids past a moving inclined plate." (2022). https://doi.org/10.21833/ijaas.2023.03.013

[18] Mutuku, Winifred Nduku, and Oluwole Daniel Makinde. "Hydromagnetic bioconvection of nanofluid over a permeable vertical plate due to gyrotactic microorganisms." *Computers & Fluids* 95 (2014): 88-97. https://doi.org/10.1016/j.compfluid.2014.02.026

[19] Singh, S. P., and Priyanka Singh. "Effect of temperature and light on the growth of algae species: A review." *Renewable and sustainable energy reviews* 50 (2015): 431-444. https://doi.org/10.1016/j.rser.2015.05.024

[20] Hwang, Yongyun, and T. J. Pedley. "Stability of downflowing gyrotactic microorganism suspensions in a two-dimensional vertical channel." *Journal of Fluid Mechanics* 749 (2014): 750-777. https://doi.org/10.1017/jfm.2014.251

[21] Khan, W.A., Rashad, A.M., Abdou, M.M.M. and Tlili, I., 2019. Natural bioconvection flow of a nanofluid containing gyrotactic microorganisms about a truncated cone. *European Journal of Mechanics-B/Fluids*, *75*, pp.133-142. https://doi.org/10.1016/j.euromechflu.2019.01.002

[22] Khashi'ie, Najiyah Safwa, Norihan Md Arifin, Ioan Pop, and Roslinda Nazar. "Dual solutions of bioconvection hybrid nanofluid flow due to gyrotactic microorganisms towards a vertical plate." *Chinese Journal of Physics* 72 (2021): 461-474. https://doi.org/10.1016/j.cjph.2021.05.011

[23] Yaseen, Moh, Sawan Kumar Rawat, Nehad Ali Shah, Manoj Kumar, and Sayed M. Eldin. "Ternary hybrid nanofluid flow containing gyrotactic microorganisms over three different geometries with Cattaneo–Christov model." *Mathematics* 11, no. 5 (2023): 1237. https://doi.org/10.3390/math11051237

[24] Algehyne, Ebrahem A., Essam R. El-Zahar, Muhammad Sohail, Umar Nazir, Hussein AZ Al-Bonsrulah, Dhinakaran Veeman, Bassem F. Felemban, and Fahad M. Alharbi. "Thermal improvement in pseudo-plastic material using ternary hybrid nanoparticles via non-Fourier's law over porous heated surface." *Energies* 14, no. 23 (2021): 8115. https://doi.org/10.3390/en14238115

[25] Ishak, Siti Shuhada, Nurin Nisa Mohd Noor Azhar, Nurul Syafiqah Nazli, Mohd Rijal Ilias, Roselah Osman, Zubaidah Sadikin, Abdul Rahman Mohd Kasim, and Nurul Farahain Mohammad. "Carbon Nanotubes Flow on Mixed Convection of Aligned Magnetohydrodynamics over a Static/Moving Wedge with Convective Boundary Conditions." *CFD Letters* 15, no. 7 (2023): 74-91. https://doi.org/10.37934/cfdl.15.7.7491

[26] Zukri, Norsyasya Zahirah Mohd, Mohd Rijal Ilias, Siti Shuhada Ishak, Roselah Osman, Nur Asiah Mohd Makhatar, and Mohd Nashriq Abd Rahman. "Magnetohydrodynamic Effect in Mixed Convection Casson Hybrid Nanofluids Flow and Heat Transfer over a Moving Vertical Plate." *CFD Letters* 15, no. 7 (2023): 92-111. https://doi.org/10.37934/cfdl.15.7.92111

[27] Ab Raji, Nurul Hidayah, Nurul Samiha Mohd Shahabudin, Noorehan Awang, Mohd Rijal Ilias, and Siti Shuhada Ishak. "Aligned Magnetohydrodynamics Mixed Convection on Various Base Fluids with Carbon Nanotubes over an Inclined Plate." *CFD Letters* 15, no. 6 (2023): 12-25. https://doi.org/10.37934/cfdl.15.6.1225

[28] Vajravelu, K., and J. Nayfeh. "Hydromagnetic convection at a cone and a wedge." *International communications in heat and mass transfer* 19, no. 5 (1992): 701-710. https://doi.org/10.1016/0735-1933(92)90052-J

[29] Batool, Maria, and Muhammad Ashraf. "MHD Nanofluid Flow with Gyrotactic Microorganisms on a Sheet Embedded in a Porous Medium." *Iranian Journal of Chemistry and Chemical Engineering* 40, no. 5 (2021): 1693-1702.
[30] Alharbi, F. M., Muhammad Naeem, Muhammad Zubair, Muhammad Jawad, Wajid Ullah Jan, and Rashid Jan. "Bioconvection due to gyrotactic microorganisms in couple stress hybrid nanofluid laminar mixed convection incompressible flow with magnetic nanoparticles and chemical reaction as carrier for targeted drug delivery through porous stretching sheet." Molecules 26, no. 13 (2021): 3954. https://doi.org/10.3390/molecules26133954
[31] Asjad, Muhammad Imran, Noman Sarwar, Bagh Ali, Sajjad Hussain, Thanin Sitthiwirattham, and Jiraporn Reunsumrit. "Impact of bioconvection and chemical reaction on MHD nanofluid flow due to exponential stretching sheet." Symmetry 13, no. 12 (2021): 2334https://doi.org/10.3390/sym13122334
[32] Soid, Siti Khuzaimah, Afiqah Athirah Durahman, Nur Hazirah Adilla Norzawary, Mohd Rijal Ilias, and AmirahMohamad Sahar. "Magnetohydrodynamic of Copper-Aluminium of Oxide Hybrid Nanoparticles Containing Gyrotactic Microorganisms over a Vertical Cylinder with Suction." Journal of Advanced Research in Applied Sciences and Engineering Technology 28, no. 2 (2022): 222-234. https://doi.org/10.37934/araset.28.2.222234
[33] Zafar Mahmood, Zahoor Iqbal, M. Alyami, Bader Alqahtani, M. Yassen and U. Khan. "Influence of suction and heat source on MHD stagnation point flow of ternary hybrid nanofluid over convectively heated stretching/shrinking cylinder." Advances in Mechanical Engineering, 14 (2022). https://doi.org/10.1177/16878132221126278.
[34] Nur Suhaida Aznidar Ismail, Ahmad Sukri Abd Aziz, M. R. Ilias and S. K. Soid. "MHD Boundary Layer Flow in Double Stratification Medium." Journal of Physics: Conference Series, 1770 (2021). https://doi.org/10.1088/1742-6596/1770/1/012045.
[35] M. R. Ilias, N. A. Rawi and S. Shafie. "MHD Free Convection Flow and Heat Transfer of Ferrofluids over a Vertical Flat Plate with Aligned and Transverse Magnetic Field." Indian journal of science and technology, 9 (2016). https://doi.org/10.17485/IJST/2016/V9I36/97347.
[36] Hamdan, Fakhru Ridhwan, Mohamad Hidayad Ahmad Kamal, Noraihan Afiqah Rawi, Ahmad Qushairi Mohamad, Anati Ali, Mohd Rijal Ilias, and Sharidan Shafie. "G-jitter free convection flow near a three-dimensional stagnation-point region with internal heat generation." *Journal of Advanced Research in Fluid Mechanics and Thermal Sciences* 67, no. 1 (2020): 119-135.
[37] Rawi, Noraihan Afiqah, Mohd Rijal Ilias, Lim Yeou Jiann, Zaiton Mat Isa, and Sharidan Shafie. "The effect of copper nanoparticles on mixed convection flow of jeffrey fluid induced by g-jitter." *Journal of Nanofluids* 7, no. 1 (2018): 156-162. https://doi.org/10.1166/jon.2018.1433
[38] Ishak, Siti Shuhada, Nurul Nurfatihah Mazlan, Mohd Rijal Ilias, Roselah Osman, Abdul Rahman Mohd Kasim, and Nurul Farahain Mohammad. "Radiation Effects on Inclined Magnetohydrodynamics Mixed Convection Boundary Layer Flow of Hybrid Nanofluids over a Moving and Static Wedge." *Journal of Advanced Research in Applied Sciences and Engineering Technology* 28, no. 3 (2022): 68-84. https://doi.org/10.37934/araset.28.3.6884
[39] Kamis, Nur Ilyana, Noraihan Afiqah Rawi, Lim Yeou Jiann, Sharidan Shafie, and Mohd Rijal Ilias. "Thermal Characteristics of an Unsteady Hybrid Nano-Casson Fluid Passing Through a Stretching Thin-Film with Mass Transition." *Journal of Advanced Research in Fluid Mechanics and Thermal Sciences* 104, no. 2 (2023): 36-50. https://doi.org/10.37934/arfmts.104.2.3650
[40] Kamal, Mohamad Hidayad Ahmad, Noraihan Afiqah Rawi, Mohd Rijal Ilias, Anati Ali, and Sharidan Shafie. "Effect of thermal radiation on a three-dimensional stagnation point region in nanofluid under microgravity environment." *Universal Journal of Mechanical Engineering* 7 (2019): 272-284. https://doi.org/10.13189/ujme.2019.070504
[41] Dolui, Soumini, Bivas Bhaumik, and Soumen De. "Combined effect of induced magnetic field and thermal radiation on ternary hybrid nanofluid flow through an inclined catheterized artery with multiple stenosis." *Chemical Physics Letters* 811 (2023): 140209. https://doi.org/10.1016/j.cplett.2022.140209
[42] Jakeer, Shaik, S. R. R. Reddy, A. M. Rashad, M. Lakshmi Rupa, and C. Manjula. "Nonlinear analysis of Darcy-Forchheimer flow in EMHD ternary hybrid nanofluid (Cu-CNT-Ti/water) with radiation effect." *Forces in Mechanics* 10 (2023): 100177. https://doi.org/10.1016/j.finmec.2023.100177
[43] Shamshuddin, M. D., Nevzat Akkurt, Anwar Saeed, and Poom Kumam. "Radiation mechanism on dissipative ternary hybrid nanoliquid flow through rotating disk encountered by Hall currents: HAM solution." *Alexandria Engineering Journal* 65 (2023): 543-559. https://doi.org/10.1016/j.aej.2022.10.021
[44] Souayeh, Basma, and Ramesh, Katta. "Numerical Scrutinization of Ternary Nanofluid Flow over an Exponentially Stretching Sheet with Gyrotactic Microorganisms." *Mathematics* 11, no. 4 (2023): 981. https://doi.org/10.3390/math11040981
[45] Tiwari, R.K., Das, M.K., Heat transfer augmentation in a two-sided lid-driven differentially heated square cavity utilizing nanofluids, International Journal of Heat and Mass Transfer, 50(9-10), 2007, 2002-2018. https://doi.org/10.1016/j.ijheatmasstransfer.2006.09.034

[46] Buongiorno, J., Convective transport in nanofluids, Journal of Heat Transfer, 128(3), 2006, 240-250. https://doi.org/10.1115/1.2150834
[47] Shampine, Lawrence F., Lawrence F. Shampine, Ian Gladwell, and S. Thompson. *Solving ODEs with MATLAB*. Cambridge university press, (2003). https://doi.org/10.1017/CBO9780511615542
[48] Ghalambaz, M., Noghrehabadi, A., & Ghanbarzadeh, A. (2014). Natural convection of nanofluids over a convectively heated vertical plate embedded in a porous medium. *Brazilian Journal of Chemical Engineering*, *31*, (2014):413-427. https://doi.org/10.1590/0104-6632.20140312s00001956
[49] Jeptoo, Chebii Agnes. "MHD Nanofluid Bioconvection Due to Gyrotactic microorganisms Past a convectively heated vertical plate." *IOSR Journal of Mathematics* 15 (2019): 50-71.
[50] Babu, M. J., Sandeep, N., & Saleem, S. Free convective MHD Cattaneo-Christov flow over three different geometries with thermophoresis and Brownian motion. *Alexandria Engineering Journal*, *56*(4), (2017):659-669. https://doi.org/10.1016/j.aej.2017.01.005
[51] Rout, B. R., S. K. Parida, and S. Panda. "MHD heat and mass transfer of chemical reaction fluid flow over a moving vertical plate in presence of heat source with convective surface boundary condition." *International Journal of Chemical Engineering* 2013 (2013). https://doi.org/10.1155/2013/296834